Fossil hydrothermal sulfide deposits at the Galapagos Spreading Centre near 85°00 West: geological setting, mineralogy and chronology

Galapagos Spreading Centre
Fossil hydrothermal sulfides
Sulfide chronology
Age of deposits/
Tectonic relation

Centre de dérive des Galapagos
Sulfures hydrothermaux fossiles
Chronologie des sulfures
Relation âge des dépôts/
Tectonique

Claude LALOU [a], Evelyne BRICHET [a], Joachim LANGE [b]

[a] Centre des Faibles Radioactivités, Laboratoire mixte CNRS/CEA, Domaine du CNRS, avenue de la Terrasse, 91198, Gif-sur-Yvette Cedex, France

[b] Preussag Aktiengesellschaft, Postfach 4829, Artnstrasse 1, Hannover 1, FRG.

Received 30/5/88, in revised form 11/8/88, accepted 29/8/88.

ABSTRACT

In the context of the Garimas (Galapagos Rift massive sulfides) project, R/V Sonne has extensively studied a segment of the Galapagos Rift from 85°50 to 85°59, and found a large number of hydrothermal fossil deposits. Two locations around 85°51 and 85°55 have been intensively sampled in a detailed navigation network. The sulfide deposits amount to some 100,000 metric tons and consist of chimney-like formations, hydrothermal crusts and ore bodies. There is no sign of present activity, but the presence of specific hydrothermal biotopes around fissures in the basement indicates that at least low-temperature emissions may be present. The mineral constituents are those commonly found in such deposits. In some samples, the two base metals, Zn and Co, reach very high concentrations. In two areas, zone A around 85°50.75 (6 samples) and zone B around 85°54.70 (25 samples), non-altered sulfide samples have been age-dated using the $^{230}Th/^{234}U$ method.

In zone B, two groups of ages are found, around 8,000 and 12,000 years, which may explain the topographic features. In zone A, only the older class (circa 12,000 years) is present. In the two zones, distance to the active accretion rate and ages are compatible with the half-spreading rate of the general area.

Oceanol. Acta, 1989, **12**, 1, 1-8.

RÉSUMÉ

Dépôts de sulfures hydrothermaux du centre de dérive des Galapagos vers 85°00 W: cadre géologique, minéralogie et chronologie

Dans le cadre du projet Garimas (Galapos Rift Massive Sulfides) le R/V Sonne a étudié de façon très détaillée le segment du Rift des Galapagos qui va de 85°50 à 85°59 Ouest, et a trouvé de nombreux dépôts hydrothermaux fossiles. Deux zones autour de 85°51 et 85°55 ont été particulièrement échantillonnées en utilisant un réseau de navigation très précis. Les dépôts de sulfure peuvent atteindre plusieurs centaines de milliers de tonnes métriques. Ils comprennent des formations semblables à des cheminées, des croûtes ou des dépôts hydrothermaux de minerai. Il n'y a pas de signe d'activité actuelle, toutefois la présence autour de fissures de communautés hydrothermales est au moins le témoin d'une activité de basse température. Les constituants minéraux sont ceux que l'on rencontre couramment dans de tels dépôts, mais les deux métaux Zn et Co peuvent atteindre de très fortes concentrations. Dans deux zones, la zone A, vers 85°50.75 (6 échantillons) et la zone B vers 85°54.70 (25 échantillons) des sulfures non altérés ont été datés par la méthode $^{230}Th/^{234}U$. Dans la zone B, les âges peuvent être regroupés en deux classes, l'une autour de 8 000 ans, l'autre autour de 12 000 ans, ce qui peut expliquer la topographie de détail de la zone. Dans la zone A, seuls les âges les plus vieux sont présents, autour de 12 000 ans et même plus. Dans les deux zones, la distance à l'axe d'accrétion et les âges sont compatibles avec la demi vitesse d'expansion de 3,5 cm/an donnée pour cette région.

Oceanol. Acta, 1989, **12**, 1, 1-8.

INTRODUCTION

The Galapagos Spreading Centre (GSC) is the first area where presently active deep-sea hydrothermal circulation has been visually observed using a submersible (Corliss *et al.*, 1979). The diving area was located around 86°10′ W and 0°47′.50 N in the rift valley, where the half spreading rate, determined from magnetic anomalies, is 35 mm/year (Sclater, Klitgord, 1973; Williams *et al.*, 1974). In this area, only relatively low-temperature vents have been found, ranging from 7°C to about 27°C in an ambient water temperature of 2.0°C (Corliss *et al.*, 1979). From these vents, the fluid is sometimes materialized by a faint milky white precipitate, and the hydrothermal deposit takes the form of manganese oxide (Corliss *et al.*, 1979). Moreover, an area of hydrothermal activity was located south of the spreading axis where the main hydrothermal deposits were nontronite, manganese and iron oxides, on a crust from 500 to 700,000 years old, representing relatively low temperature deposits (Corliss *et al.*, 1979). From chemical considerations on the composition of the water issuing from the active vents in the rift valley, it was concluded that interactions between the water and rocks may occur at a temperature of at least 300°C (Corliss *et al.*, 1979).

Some hydrothermal deposits, essentially Mn and Fe oxides, were previously observed and sampled in the Atlantic Ocean (Arcyana, 1974; Scott *et al.*, 1974), but there was no evidence of the presumed high temperature hydrothermal activity until the discovery of fossil polymetallic hydrothermal sulfides (Francheteau *et al.*, 1979), followed by the discovery of their genitors, the black smokers, at 21°N on the East Pacific Rise (Hékinian *et al.*, 1980). These discoveries opened a new field in geological, chemical and biological oceanography, with the result that numerous diving cruises have been devoted to the search for new areas of hydrothermalism along the ocean-ridge system; numerous indications of high temperature hydrothermalism are currently found in the Atlantic as well as in the Pacific Ocean.

In the course of the Galapagos Rift And Fracture Zone Intersection (GRAFZI) project in 1980, Alvin dives allowed Malahoff *et al.* (1983) to discover inactive fossil

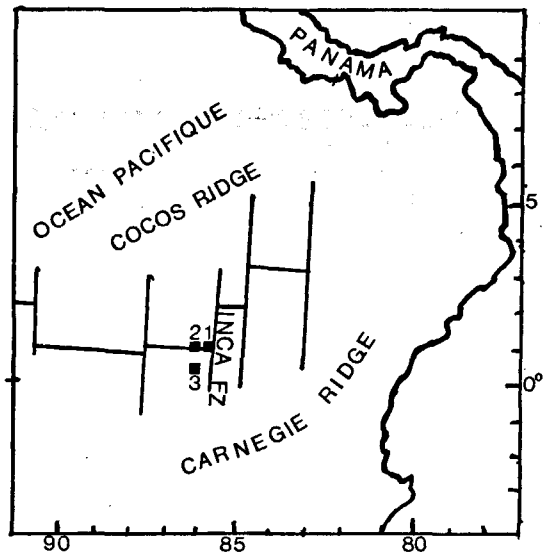

Figure 1

General map of the East Equatorial Pacific showing the areas where hydrothermal activity near the Galapagos Spreading Centre has been identified. 1) *Present study (high temperature fossil sulfides);* 2) *Presently active low temperature vents (Corliss* et al., 1979); 3) *Hydrothermal mounds (iron silicates, manganese oxides) (Corliss* et al., 1979).

Carte générale du Pacifique Est Équatorial montrant les zones où une activité hydrothermale a été détectée près du Centre de dérive des Galapagos. 1) Cette étude (sulfures fossiles de haute température); 2) Sources hydrothermales actives de basse température (Corliss *et al.*, 1979); 3) Monts hydrothermaux (silicates de fer, oxydes de manganèse) (Corliss *et al.*, 1979).

mounds of sulfide at 86°W in the Galapagos Rift; these mounds have been shown as deposited at a temperature of 390° ± 20°C (Skirrow, Coleman, 1982).

In the GARIMAS ("Galapagos Rift Massive Sulfides") project, two economically oriented research cruises took place in 1984 and 1985 with the German research vessel Sonne, during which the Galapagos Rift between the Inca Fracture Zone and the De Steiguer Deep was mapped and surveyed by a deep-towed televison camera system. An extensive study of the segment from 85°50 to 85°59 was carried out (Fig. 1), and led to the discovery of a large number of fossil deposits (Fig. 2). They show a great variety of types, including massive sulfide deposits, mounds composed of Fe- and Mn-oxyhydroxides and chimney fields almost entirely formed of amorphous silica.

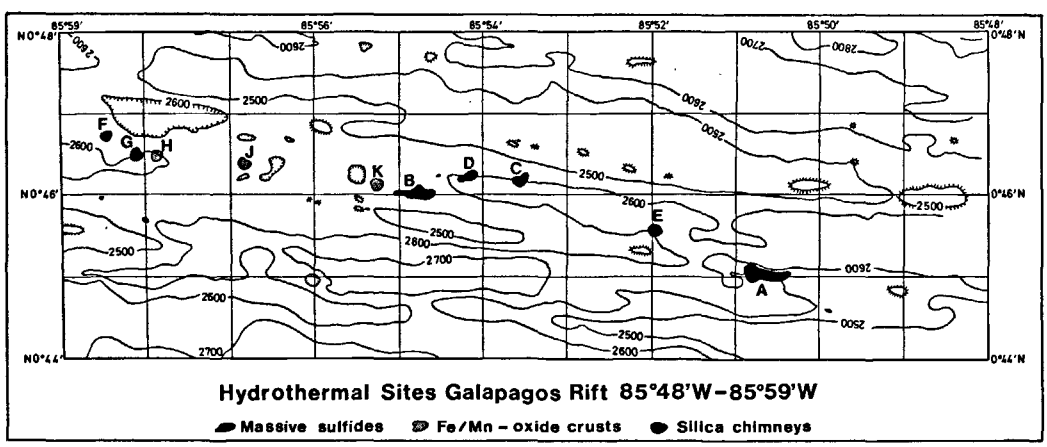

Figure 2

Hydrothermal sites, Galapagos Rift from 85°48′W to 85°59′W. The samples for this study come from zones A and B.

Sites hydrothermaux dans le «rift» des Galapagos entre 85°48′ Ouest et 85°59′ Ouest. Les échantillons étudiés ici viennent des zones A et B.

The detailed survey conducted by the R/V Sonne made use of the following navigation systems: a) GPS (Global Positioning System) satellite navigation; b) ATNAV bottom transponder navigation; and c) a Honeywell RS 904 ultra-short-base positioning system for the towed vehicles. The accuracy of the sample location is estimated at 75±25 m. Bathymetric mapping was done with a Seabeam system and a stabilized 20 kHz narrow-beam echo sounder.

Based on bathymetric maps, combined television and photographic profiles were run, employing the Preussag Ocean Floor Observation System (OFOS).

Sulfides were recovered by the Preussag electro-hydraulic grab equipped with TV camera. Televisual observation of the sea floor makes it possible to distinguish between basalts and ore outcrops. When sulfides were recognized on the on-board monitor, the TV grab was lowered to the seafloor and closed by an electrical release command. With such an apparatus, the position of the samples is more accurately established than with conventional dredging techniques.

Two areas at a depth of about 2,600 m have been extensively sampled and studied: area A around 85°50′70 W, 0°45′0 N, and area B around 85°54′80 W, 0°45′70 N. One sulfide sample from station F, 85°58′43 W, 0°46′72 N has also been studied.

Table 1 gives the position of all dated samples.

The purpose of this study is, by dating the sulfide deposits, to provide a time scale for the hydrothermal processes that took place in this area in relation to its geological setting.

Table 1
Position of the stations where sulfides have been dated.
Position des échantillons de sulfures qui ont été datés.

Sample N°	Station N°	Latitude North	Longitude West
Zone A			
A CS 1	49 GTV	0°45.07	85°50.74
A CS 2	46 GTV	.00	.61
A CS 3	72 GTV	.00	.64
A CS 4	65 GTV	.01	.71
A CS 9	136 DC	44.96	.81
A MFM15	61 GTVC	45.00	.49
Zone B			
B CS19	139 DC	0°46.08	85°54.84
B CS20	158 DC	46.02	88
B CS21	161 DC	45.93	92
B MFM32	202 GTVA	46.056	78
B MFM34	213 GTVC	45.978	60
B MFM 9	50 GTVC	46.015	64
B MFM25	127 GTVC	45.99	77
B MFM12	56 GTVC	99	67
B MFM20	112 GTVB	99	84
B MFM23	121 GTVA	97	69
B MFM26	146 GTVC	98	78
B MFM33	207 GTVA	46.04	59
B MFM30	185 GTVA	17	69
B MFM11	55 GTVC	45.98	71
B DSB37	117 GTVB	46.00	59
B MFM28	170 GTVB	04	95
B MFM35	215 GTVC	12	74
B DSB 2	11 GTVC	45.94	75
B MFM16	65 GTVC	46.00	87
B MFM13	58 D	45.998	74
B DSB30	60 GTVC	96	75
B MFM6	42 GTVC	99	63
B MFM27	169 GTVB	46.00	70
B DSB38	120 GTVA	45.985	663
B DSB52	171 GTVB	963	603
Zone F (?)			
F FMF36	228 GTVC	46.724	85°58.435

GEOLOGICAL SETTING AND TYPE OF HYDROTHERMAL MINERALIZATIONS (85°48′W TO 85°59′W)

The structural trend of the Galapagos Rift in the segment investigated is characterized by a pronounced axial valley at 2 550-2 660 m depth. The marginal walls climb to 2 400 m in the north and 2 460 m in the south.

Despite characteristic morphological differences, the axis and adjacent areas of the generally 96°—striking Galapagos Rift system display several comparable structural units for the two areas investigated in detail (A and B). The marginal height is bordered on the south by the northern rift valley, followed by the main central horst structure, the southern rift valley and finally the southern marginal height. The active spreading axis of the rift system is incorporated into the northern rift valley, which in turn can be further subdivided.

The occurrence of hydrothermal activity in general and of massive sulfide deposits in particular points to an origin of hydrothermal metallogenesis in relation to certain types of fluid basalts as well as to active tensional stresses.

The sampling locations were situated slightly to the south (0.5 to 0.9 km) of the recent axis of accretion. Site A, first described by Malahoff (1982), is located at the top and at the southern base of a central horst structure marking the axis of symmetry of a double rifted valley from 85°50′W to 85°51′W. Site B was detected during the GARIMAS 1 cruise and is situated at the northern base of the central horst structure, bordering the recently active northern rift valley between 85°54′W and 85°55′W.

The main area surveyed by photographic profiles extends from 85°50′ to 85°59′W, and covers mainly the massive sulfide deposits at location B (85°54.5-85°55′W) and its eastern and western prolongation. The results obtained demonstrate that the sulfide occurrences cover an area 650 m in length and some 100 m in width. Individual outcrops were observed outside this area. The presence of sulfides at location B is connected to distinct tectonic lineaments, striking quite parallel to the rift axis and marginal faults of the rift valley. Massive sulfide outcrops at location B are partially associated with larger Fe/Mn-oxide stacks of primary low-temperature origin. In addition, Fe-silicate edifices were observed, showing similar shapes and sizes as sulfide outcrops. Besides detailed photoprofiling at location B, profiles were placed at location A (85°50′W) to supplement data gathered during GARIMAS 1. The photographic profiles located outside detail areas A and B resulted in the detection of 8 new hydrothermal fields (C-K, *see* Fig. 2). Locations E and F consist of sulfide stacks, slightly oxidized at the surface. At location E, these stacks are situated within a talus slope; at location F they are rooted at the boundary of fresh nodular sheet lava and old pillow lava terrain. The high diversity of products occurring at hydrothermal sites was demonstrated by the detection of pure amorphous silica chimneys at locations C, D, G and hydrothermal mound assemblages (H, J, K) consisting of Fe-

Mn-oxide mineralizations, mostly forming edifices of layered or crust-like structures. While locations C and D have been found at the base of the axial valley bordering northern fault scarp, sites E, G, H, J and K seem to be located on a lineament striking 95° in prolongation of the B occurrence. Only site F is situated at the slope of an axial volcanic cone.

CHARACTERIZATION OF MASSIVE SULFIDE MINERALIZATIONS (SITES A AND B)

Individual deposits of massive sulfides differ in shape and can amount to some 10,000 metric tons. Chimney-like formations up to several metres height exist around the vents of thermal springs, as well as crusts up to several centimetres thick and ore bodies covering relatively large surface areas.

Evidence of recent thermal spring activity on the ocean floor of hydrothermal solutions jetting out of the massive sulfide ore bodies could not be found in either of the two investigated areas. This indicates that the massive sulfide deposits in question are already inactive. Halmyrolitic alteration products belonging to massive sulfide deposits (limonite) add further support to this conclusion. Although there is no evidence of direct emission from thermal springs at either location, signs of recent hydrothermal activity can be observed. Indications are given by the sudden appearance of numerous organisms, that is to say by faunal associations (*e.g.* crustaceans, bivalves, worms) characteristic of biotopes around fissures which often serve as feeder channels for hydrothermal vents.

The samples of complex massive sulfide ores recovered are portions of black smokers. A characteristic aspect of these massive sulfide ores is generally a macroscopically as well as microscopically conspicuous porous, layered compositional structure, with occasional obvious zonal arrangements of sulfides.

In some fragments, predominantly within marginal parts of the samples, relicts of organisms such as worm tubes reaching more than one centimetre in diameter are embedded in the sulfide minerals. These relicts provide a document of the fantastically abundant fauna present in the vicinity of "black smokers" and "white smokers".

The mineralogical composition of the fragments reveals the presence of extremely heterogeneous sulfide mineralizations, with consequent marked variations in their chemical composition. This applies to the main elemental constituents (iron, zinc and copper) as well as to trace elements. There is an extremely wide range of variation in zinc and copper content with occasional very high concentrations, especially in the case of zinc, which varies from 0.2 to 34.2% in area B.

The considerable variety of the mineralogical composition is seen in the fact that the major constituents, sulfides of iron, zinc and copper, are present in widely differing relative proportions. Sporadically, some of these sulfides may appear diminished in such a manner that, in the respective massive sulfide mineralizations, they rank as no more than accessory constituents. These variations can occur within a narrow spatial range. Additionally, fragments belonging to different mineralogical formations were also sampled from a single locality. Fragments have been extracted which consist of almost pure iron sulfide (pyrite in several generations and different external forms). On the other hand, complex massive sulfide ores show in places, apart from their high iron content, substantial amounts of copper and/or zinc. Portions of "black smokers" can also be observed which frequently contain extreme zinc enrichments.

As these complex massive sulfide ores often exhibit zonal structures, they may be variations in the relative proportions of the constituents in the very same formation. It becomes obvious from these facts that a quantitatively precise determination of the mineralogical and chemical composition of the respective sulfide mineralizations, recovered only in fragments, appears to be out of the question as long as representative sampling of the deposits remains impossible.

Major mineral constituents of the complexe massive sulfide ores are pyrite, melnikovite-pyrite, marcasite, chalcopyrite, sphalerite, wurtzite and schalenblende. In place, these sulfides may be diminished to the state of only minor or even accessory mineral constituents within these hydrothermal mineralizations. Very common and extremely characteristic for the complex massive sulfide ores are colloidal and/or gel textures, represented essentially by pyrite, melnikovite-pyrite, marcasite and schalenblende, and locally even by covellite. Furthermore, sphalerite quite frequently appears in dendritic to "knitted" aggregates and in these formations is partly paraamorphous after wurtzite and schalenblende.

In addition to a very rich yield of complex massive sulfide ores in both areas investigated, further types of sulfide mineralizations were discovered. Sulfide crusts exist on volcanic rocks and also veinlets, joints and fissures filled with sulfides, as well as fragments and breccias, of volcanic rocks cemented by sulfides ("hydrothermal breccias"). Additionally, volcanic rocks have been recovered which may exhibit a certain ore content (*e.g.* sulfide impregnations).

AGE-DATING TECHNIQUE AND SAMPLE PREPARATION

As already pointed out, three areas of hydrothermal events have been found in the Galapagos Rift. From a chronological point of view, it is known that the area found in the rift around 86°W is in the course of formation, and that the Galapagos mounds have formed relatively continuously from 600,000 years to the present (Lalou *et al.*, 1986). As far as the presently described area is concerned, it appeared of interest to make a chronological study of the sulfide samples obtained which present well-preserved and non-oxidized parts, in order to determine whether they represent an isolated event or a series of discrete events.

The use of uranium series disequilibrium to date hydrothermal deposits has proved reliable (Lalou, Brichet, 1987). Depending on the age and duration of the phenomenon, three time-scales are available: 0-15

years, using $^{228}Th/^{228}Ra$; 0-200 years, using $^{210}Pb/Pb$; and 5000-350,000 years, using $^{230}Th/^{234}U$. The methods have been established and applied to the 21°N and 12°50 N EPR sulfide presently forming at the axis of the rift valley and to inactive sulfide deposits on off-axial structures (Lalou, Brichet, 1980; 1982; Lalou *et al.*, 1985).

Preliminary measurements performed on a number of samples to select the appropriate method have shown that the ^{210}Pb activity present in the samples is due only to the decrease of ^{230}Th, that is endogeneously built, and not coming with stable lead from the hydrothermal fluid; the samples are thus certainly older than 200 years and the $^{230}Th/^{234}U$ method should be applied: indeed, it is the only possible one.

Sample preparation

From massive pieces of sulfide, subsamples have been separated, from the central part, to avoid any trace of oxidation. This is done because, in the process of oxidation, sulfides concentrate uranium from ambient sea water, resulting in an apparent younger age. Generally, the uranium content of sulfides is lower than about 2 ppm. Samples are then crushed and a mineralogical determination is made using X-ray diffraction.

Radiochemical analyses are carried out on 2-8 g of the powdered sample following the procedure of Ku (1976), slightly modified for application to this special material: An HCl, 8 N + HNO_3, 8 N mixture with addition of $HClO_4$ is used to solubilize the sample, any insoluble residue being solubilized in a concentrated $HNO_3 + HClO_4 + HF$ mixture. ^{228}Th in equilibrium with its parent ^{232}U was used as a spike and introduced at the beginning of the operations. Alpha activity measurements were made by alpha spectrometry using either solid state detectors or a gridded ion chamber.

GEOCHRONOLOGY OF THE SULFIDES

Radiochemical results are presented in Table 2 with the calculated ages. Errors given on the ages are statistical counting errors at 1 σ level. Mineralogical composition of the dated subsamples is shown in order of decreasing abundance. One characteristic that permits confidence in the ages is that no inverse correlation between uranium content and ages exists that would be indicative of a postdepositional introduction of uranium making samples appear younger (Lalou, Brichet, 1987). As seen in Figure 3, which shows age as a function of the uranium content, such a relation does not exist; moreover, samples with very different uranium content (depending probably on their mineralogical characteristics) present quite identical ages.

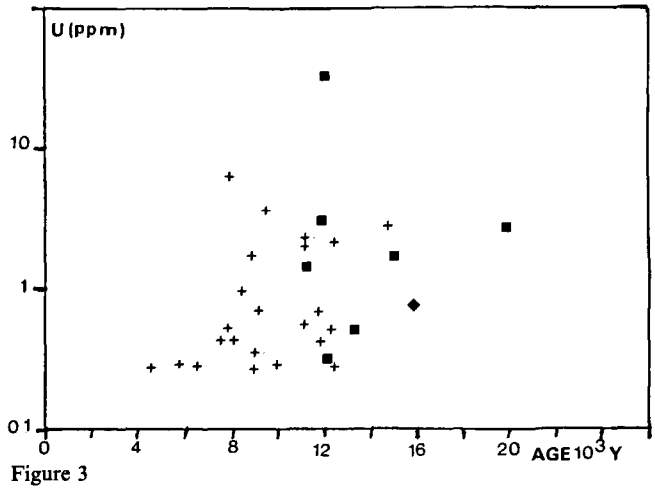

Figure 3

Age of the samples as a function of uranium content showing that there is no inverse correlation between ages and U contents. Squares are for zone A samples, crosses are for zone B and diamonds for zone F.

Age des échantillons en fonction de leur teneur en uranium montrant qu'il n'y a pas de corrélation inverse entre l'âge et la teneur en uranium. Les carrés représentent les échantillons de la zone A, les croix ceux de la zone B, le losange celui de la zone F.

Figure 4 is a frequency histogram of all the ages for the three studied zones, constructed from Table 2. From this, two groups of ages are roughly determined, one centered around 8,000 years, only present in zone B, the other around 12,000 years, present in both areas (A and B), with possibly an older event represented by too few samples to be statistically valuable. To evaluate whether these age groups have a meaning on the geographical and/or topographical scale. On Figure 5 are reported the ages of the samples on a large scale map for zone B where the samples are more numerous; the same is done in Figure 6 for zone A.

More samples adapted for the chronological study were available in zone B, thanks to the second Sonne cruise, as a result of which it was possible to obtain samples preserved from crushing on board, permitting selection of the freshest non-oxidized parts for dating. All samples show the low uranium content and very low ^{232}Th content characteristic of non-altered sulfide deposits

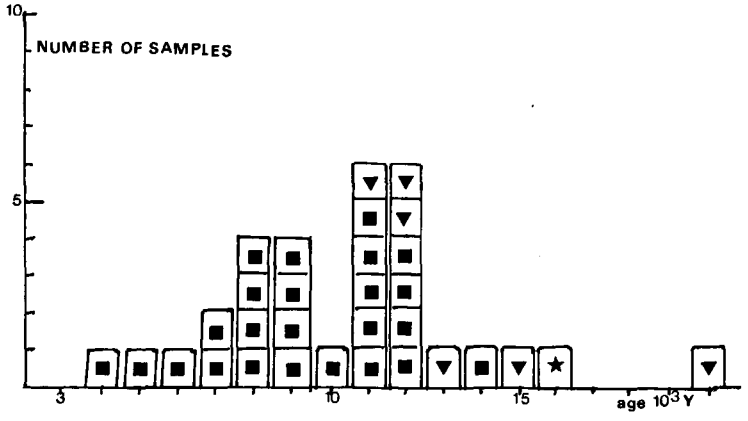

Figure 4

Histogram of the ages of sulfide deposits. Squares = zone B; triangles = zone A; star = zone F.

Histogramme donnant les âges des dépôts de sulfures en fonction du nombre de fois où cet âge est trouvé, carrés = zone B; triangles = zone A; étoile = zone F.

Table 2

Mineralogy and radiochemical results of sulfide samples from the three studied zones. Errors are statistical counting errors at 1 sigma level.

Minéralogie et résultats de l'analyse radiochimique pour les échantillons de sulfures des trois zones étudiées. Les erreurs sont les erreurs

Station	Mineralogy	U-238 (ppm)	U-234 (dpm/g)	234/238	Th-230 (dpm/g)	Th-232 (ppm)	230/234	Age (10^3 y)
Zone A								
61 GTVC	Pyrite	1.717	1.490	1.179	0.191	0.040	0.128	15 ±1.5
MFM 15	Marcasite Chalcopyrite	±0.045	±0.038	±0.025	±0.016	±0.013	±0.011	
46 GTV	Pyrite	33	27.4	1.137	2.89	0.21	0.106	12.1 ±0.6
CS2	Marcasite Chalcopyrite	±1	±0.9	±0.037	±0.09	±0.02	±0.005	
49 GTV	Pyrite	0.53	0.43	1.103	0.050	<0.006	0.116	13,3 ±1.3
CS1	Chalcopyrite Sphalerite (?)	±0.02	±0.013	±0.02	±0.005		±0.011	
72 GTV	Pyrite	1.51	1.26	1.136	0.125	<0.005	0.099	11.3 ±0.7
CS3	Sphalerite Chalco. Marc. amorph. silica	±0.04	±0.04	±0.03	±0.006		±0.006	
65 GTV	Pyrite	0.31	0.261	1.147	0.028	<0.006	0.107	12.25±1.25
CS4	Chalco. Marc.	±0.01	±0.008	±0.047	±0.002		±0.010	
136 DC		2.73	2.31	1.150	0.40	0.38	0.173	20.5 ±1.9
CS9		±0.11	±0.09	±0.06	±0.03	±0.05	±0.014	
Zone B								
202	Chalcopyrite	0.438	0.342	1.063	0.025	0.006	0.072	
MFM 32	Pyrite amorph. Silica	±0.033	±0.025	±0.090	±0.004	±0.003	±0.011	8.1 ±1.3
213	Chalcopyrite							
MFM 34	Marcasite Pyrite amorph. Silica	0.296 ±0.014	0.237 ±0.011	1.092 ±0.064	0.026 ±0.005	0.014 ±0.006	0.108 ±0.019	12.4 ±2.4
50	Sphalerite	0.521	0.399	1.041	0.028	0.002	0.070	7.9 ±0.8
MFM 9	Pyrite Chalcopyrite amorph. Silica	±0.021	±0.016	±0.045	±0.003	±0.001	±0.007	
127	Chalcopyrite							
MFM 25	Marcasite Pyrite amorph. Silica	1.689 ±0.060	1.426 ±0.049	1.147 ±0.032	0.112 ±0.008	0	0.079 ±0.006	8.9 ±0.7
56	Pyrite	1.061	0.833	1.067	0.194	0.525	0.233	<30
MFM 12	Chalcopyrite amorph. Silica Detritic	±0.032	±0.025	±0.025	±0.009	±0.027	±0.013	
112	Chalcopyrite	2.270	1.892	1.132	0.188	0	0.099	11.3 ±1.1
MFM 20	Pyrite Sphalerite	±0.059	±0.048	±0.017	±0.017		±0.009	
121								
MFM 23	Pyrite Marcasite Chalcopyrite Silica	2.008 ±0.053	1.663 ±0.043	1.125 ±0.018	0.164 ±0.006	0.005 ±0.002	0.099 ±0.005	11.3 ±0.6
146	Chalcopyrite							
MFM 26	Marcasite Pyrite Few silica	0.558 ±0.017	0.467 ±0.014	1.138 ±0.033	0.046 ±0.003	0.003 ±0.001	0.098 ±0.006	11.2 ±0.8
207	Chalcopyrite	0.530	0.417	1.070	0.045	0	0.108	12.4 ±1
MFM 33	Marcasite Pyrite amorph. silica	±0.015	±0.011	±0.029	±0.003		±0.008	

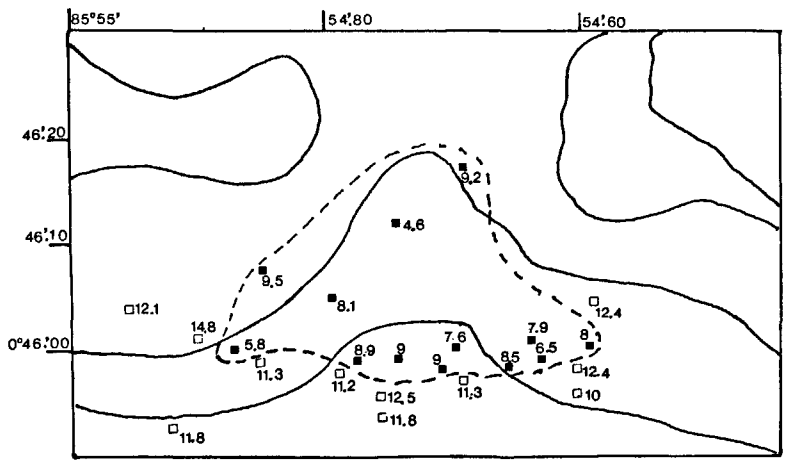

Figure 5

Map of sulfide deposits in zone B, showing ages of the deposits. The dashed line separates the <10,000 years samples from the >10,000 years ones.

Carte des dépôts de sulfures de la zone B donnant la répartition des âges. La ligne en pointillé sépare les échantillons dont l'âge est <10000 ans de ceux >10000 ans.

statistiques de comptage à 1 sigma.

Station	Mineralogy	U-238 (ppm)	U-234 (dpm/g)	234/238	Th-230 (dpm/g)	Th-232 (ppm)	230/234	Age (10^3 y)
185	Chalcopyrite	0.714	0.624	1.188	0.051	0.007	0.082	9.2 ±0.9
MFM 30	Pyrite	±0.029	±0.024	±0.042	±0.005	±0.003	±0.007	
55	Pyrite	0.274	0.234	1.160	0.019	0	0.080	9 ±1
MFM 11	Chalcopyrite Marcasite amorph. silica	±0.009	±0.007	±0.042	±0.002		±0.009	
117	Silica	6.357	5.449	1.165	0.385	0.006	0.071	8 ±0.5
DSB 37	Pyrite Chalcopyrite	±0.138	±0.117	±0.010	±0.019	±0.004	±0.004	
170	Pyrite	0.082	0.073	1.208	0.008	0	0.106	12.1 ±2.6
MFM 28	Chalcopyrite Marcasite	±0.006	±0.005	±0.115	±0.002		±0.024	
215	Chalcopyrite	0.272	0.223	1.115	0.009	0	0.042	4,6 ±1
MFM 35	Pyrite Marcasite	±0.025	±0.021	±0.123	±0.002		±0.009	
11	Pyrite	0.690	0.564	1.110	0.058	0.001	0.103	11.8 ±0.8
DSB 2	Cristobalite	±0.041	±0.032	±0.061	±0.006	±0.001	±0.006	
65	Pyrite	0.280	0.242	1.174	0.012	0.001	0.052	5.8 ±0.6
MFM 16	Cristobalite	±0.008	±0.007	±0.040	±0.001	±0.001	±0.005	
58	Silica + quartz							
MFM 13	Pyrite Chalcopyrite Marcasite Sphalérite	0.348 ±0.010	0.298 ±0.008	1.162 ±0.039	0.024 ±0.002	0.009 ±0.002	0.080 ±0.006	9.0 ±0.7
Zone B								
60	Pyrite	2.245	1.916	1.160	0.209	0.003	0.109	12.5 ±0.5
DSB 30		±0.042	±0.036	±0.014	±0.007	±0.001	±0.004	
42	Sphalérite	0.271	0.219	1.098	0.013	0	0.058	6.5 ±0.8
MFM 6	Pyrite Marcasite Chalcopyrite	±0.011	±0.009	±0.051	±0.002		±0.007	
169	Chalcopyrite	0.434	0.385	1.205	0.026	0.006	0.068	7.6 ±0.8
MFM 27	Pyrite Few Silica	±0.014	±0.012	±0.041	±0.003	±0.002	±0.007	
120	Chalcopyrite							
DSB 38	Pyrite Marcasite Sphalérite Silica (Feldspars)	0.976 ±0.022	0.821 ±0.018	1.144 ±0.023	0.062 ±0.004	0	0.075 ±0.005	8.5 ±0.6
171	Chalcopyrite							
DSB 52	Pyrite Marcasite	0.292 ±0.004	0.255 ±0.005	1.185 ±0.028	0.023 ±0.002	0	0.089 ±0.010	10.0 ±1.2
139 DC	Sphalerite	3.6	3.14	1.184	0.26	<0.012	0.084	9.5 ±0.7
CS 19	Pyrite Marc. Silica	±0.1	±0.10	±0.026	±0.016		±0.006	
158 DC	Chalcopyrite	2.77	2.27	1.115	0.290	<0.011	0.128	14.8 ±1
CS 20	Pyrite	±0.12	±0.10	±0.082	±0.017		±0.009	
161 DC	Sphalerite	0.42	0.36	1.183	0.038	–	0.104	11.9 ±2.4
CS 21	Pyrite Marc. Chalco.	±0.03	±0.03	±0.1	±0.007		±0.020	
Zone F								
228	Pyrite	0.788	0.073	1.213	0.096	0.049	0.137	16 ±4
FMF 36	Chalcopyrite	±0.041	±0.034	±0.063	±0.021	±0.028	±0.030	

Figure 6
Map of the sulfide deposits in zone A showing ages.
Carte des dépôts de sulfure de la zone A donnant leurs âges.

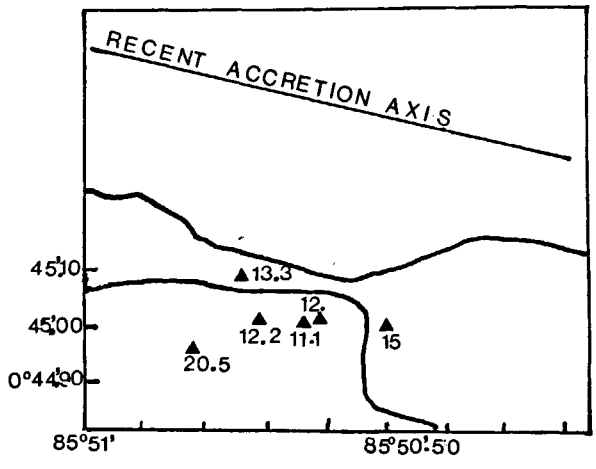

(Lalou, Brichet, 1987). The two groups of ages previously established are well evidenced, all the older ages (greater than 10,000 years) are located at the periphery of the studied zone. It is not as yet clear whether the sample dated at 9.2 10^3 years (sample 185) is related to the first or to the second event. There is no analytical reason to reject it, both uranium and ^{232}Th content being low. The best explanation for such a distribution of ages would be an old event (from about 14 to 11. 10^3 years) on which a younger event has been superimposed.

In zone A, only few samples were convenient for radiochemical measurements because on-board crushing mixed oxidized and non-oxidized parts of the samples. Only five measurements were acceptable; sample 46, which is a mixture of sulfide and oxide, is suspect due to its very high U content and relatively high ^{232}Th content, but has nervertheless been retained, as it is in the time span covered by the other neighbouring samples. As in zone B, the oldest sample is farther than the younger ones from the accretion axis. The distance between sample 136, the oldest, and the others is approximately 250 m, the difference in age being about 8,000 years. With a half-spreading rate of 3.5 cm/year, it corresponds to a distance of 280 m, which is in accordance with the relative positions of the samples. We can use the age of the main deposit (about 12,000 years) and the spreading rate (3.5 cm/year) to fix the southern boundary of this rift valley, considering that active black smokers can develop only in the active valley. This calculation situates the southernmost limit of the active valley (*i.e.* the basement of zero age) some 400 to 500 m north of the present position of the samples, which seems a good approximation in accordance with the field observation. This is in agreement with the fact that the sulfides, at this location, align along two fault scarps which follow the southern slope of what appeared to be a central height between two rift valleys.

In zone B, the same calculations lead us, if we take a mean age of 12,000 years for the oldest event, to place the southern boundary of the active valley about 400 to 450 m north of the present position of the samples, which may be roughly considered in accordance also with the emplacement of the youngest event but which once again renders questionable the age of $9.2\,10^3$ years found for sample 185.

In such an area with slow spreading rates and for young ages, it is evident that these calculations cannot be really precise because they represent distances too short to be unaffected by local tectonic events. Moreover, in contrast with what happens in subaerial regions, for which the continuity or discontinuity of formations may be ascertained, one must keep in mind that even with the relatively sophisticated underwater survey technics applied, such certainty does not exist.

CONCLUSIONS

The sulfide deposits of the Galapagos Spreading Centre are at present the largest fossil deposits found in the deep sea. Their precise study has been possible due to the sophisticated mapping and sampling methods used by R/V Sonne.

The age dating has permitted to establish the presence of two hydrothermal events, the youngest – about 8,000 years ago – being restricted to the area situated in the western part of the spreading axis, *i.e.* closer to the area of present day activity, the oldest being present in the two studied areas. On-board observations have shown that some of the zone B sulfides have a fresher appearance than those of zone A; moreover, it seems that low temperature thermal water, which cannot give sulfide deposition, and hydrothermal biological communities are present in zone B. Sample F (16 ± 4.10^3 years), closer to the present-day activity area, seems to be in opposition with this conclusion; but it is an isolated sample and this field is situated on the northern wall of the spreading axis and so probably cannot be compared to the others from the southern one. Roughly, the ages and positions of samples are in agreement with the mean half-spreading rate of the area. No relationship can at present be established between ages and mineralogy.

Acknowledgements

The authors acknowledge with thanks Preussag, which permitted the use of samples from GARIMAS 1 and GARIMAS 2 cruises of R/V Sonne. Thanks are due to two anonymous reviewers for constructive suggestions. C.L. and E.B. thank CNRS and CEA for financial support of the study. This is CFR contribution n° 976.

REFERENCES

Arcyana, 1974. Transform fault and rift valley from bathyscaph and diving saucer, *Science*, **190**, 108-116.

Corliss J. B., Dymond J., Cordon L. I., Edmond J. M., von Herzen P., Ballard R. D., Green K., Williams D., Bainbridge A., Crane K., van Andel T. H., 1979. Submarine thermal springs on the Galapagos Rift, *Science*, **203**, 1073-1083.

Francheteau J., Needham H. D., Choukroune P., Juteau T., Seguret M., Ballard R. D., 1979. Massive deep-sea sulphide ore deposits discovered on the East Pacific Rise, *Nature*, **277**, 523-528.

Hékinian R., Février M., Bischoff J. L., Picot P., Shanks W. C., 1980. Sulfide deposits from the East Pacific Rise near 21°N, *Science*, **207**, 1433-1444.

Ku T. L., 1976. The uranium series methods of age determination, *Ann. Rev. Earth Planet. Sci.*, **4**, 347-379.

Lalou C., Brichet E., 1980. Les dépôts de sulfure hydrothermaux de la Dorsale Est Pacifique à 21°N. Étude des isotopes de la famille de l'uranium, *C.R. Acad. Sci. Paris, Sér. D*, **290**, 819-822.

Lalou C., Brichet E., 1982. Age and implication of East Pacific Rise sulphide deposits at 21°N, *Nature*, **300**, 169-171.

Lalou C., Brichet E., 1987. On the isotopic chronology of submarine hydrothermal deposits, *Chem. Geol. (Isotope Geosci. Sect.)*, **65**, 197-207.

Lalou C., Brichet E., Peres-Leclaire H., 1984. The Galapagos hydrothermal mound history from about 600,000 years to present, *Oceanol. Acta*, **7**, 3, 261-270.

Lalou C., Brichet E., Hékinian R., 1985. Age dating of sulfide deposits from axial and off-axial structures of the East Pacific Rise near 12°50'N, *Earth Planet. Sci. Lett.*, **75**, 59-71.

Malahoff A., Embley R. W., Cronan D. S., Skirrow R., 1983. The geological setting and chemistry of hydrothermal sulfides and associated deposits from the Galapagos Rift at 86°W, *Mar. Min.*, **4**, 123-137.

Sclater J. G., Klitgord K. D., 1973. A detailed heat flow, topographic and magnetic survey across the Galapagos Spreading Center at 86°W, *J. Geophys. Res.*, **78**, 6951-6975.

Scott R. D., Rona P. A., Mc Gregor B. A., Scott M. R., 1974. The TAG hydrothermal field, *Nature*, **251**, 301-302.

Skirrow R., Coleman M. L., 1982. Origin of sulphur and geothermometry of hydrothermal sulphides from the Galapagos Rift, at 86°W, *Nature*, **299**, 142-144.

Williams D. L., Von Herzen R. P., Sclater J. G., Anderson R. N., 1974. The Galapagos Spreading Center: Lithospheric cooling and hydrothermal circulation, *Geophys. J. R. Astron. Soc.*, **38**, 587-608.